Transaction B: Mechanical Engineering
Vol. 16, No. 6, pp. 470–478

SCIENTIA IRANICA

Natural Convection over a Non-Isothermal Vertical Flat Plate in Supercritical Fluids

A.R. Teymourtash[1,*] and M. Ebrahimi Warkiani[1]

Abstract. *In many applications, convection heat transfer is coupled with conduction and radiation heat transfer, which generate temperature gradients along the walls and may greatly affect natural convection heat transfer. The main objective of this study is to calculate the heat-transfer characteristics for natural convection from a non-isothermal vertical flat plate into a supercritical fluid. The influence of the non-uniformity of wall temperature on the heat transfer by natural convection along a vertical plate, having a linearly distributed temperature (characterized by the slope S) is also investigated. The thermal expansion coefficient is considered as a function of the temperature, the pressure, the van der Waals constants and the compressibility factor. The trends of the curves obtained with this equation and with values from tables of thermodynamic properties were similar and diverged at a critical point. These features confirmed the validity of this equation. Then, the governing systems of partial differential equations are solved numerically using the finite difference method. The local Nusselt number was then calculated and plotted as a function of the local Rayleigh number. It was observed that a positive slope of temperature distribution increases the heat transfer rate and a negative slope decreases it.*

Keywords: *Finite difference method; Natural convection; Nusselt number; Rayleigh number; Supercritical Fluids.*

INTRODUCTION

Supercritical fluids are gases/liquids that are at temperatures and pressures above their critical points. The phenomena concerning the behavior of supercritical fluids have been the subject of research since the 1800 s. Supercritical fluids, particularly supercritical CO_2, have been used in areas ranging from materials cleaning, natural products extraction, chemical reactions, sample preparation and environmental remediation [1]. Heat transfer by natural convection applied to simple geometries, such as flat plates, spheres and cylinders, has been extensively studied for decades. Information on many topics related to supercritical fluid applications is also abundant. However, studies of natural convection in supercritical fluids are very scarce.

1. *Department of Mechanical Engineering, Faculty of Engineering, Ferdowsi University of Mashhad, Mashhad, P.O. Box 91775-1111, Iran.*
*. *Corresponding author. E-mail: teymourtash@um.ac.ir*

Received 7 July 2008; received in revised form 5 November 2008; accepted 3 January 2009

Ostrach [2] was one of the first to solve the boundary layer equations for natural convection from a vertical flat plate using a numerical method, reducing the set of three equations (continuity, momentum and energy) to only two equations with their respective boundary conditions. He found that this type of flow is dependent on the Grashof number and Prandtl number. McHugh and Krukonis [3] gave an excellent introduction to the properties and uses of supercritical fluids. Nishikawa and Ito [4] did modeling for free convection to supercritical fluids based on boundary-layer equations and similarity transformation, taking into account variable physical properties of the fluid. However, no effect of temperature on thermal expansivity was accounted for.

When the environment is isothermal and stagnant, a coordinate transformation allows simplifying the steady laminar boundary-layer equations from partial differential equations to ordinary differential equations. Sparrow and Gregg [5] gave a solution of this system in the case of exponential and power law temperature distributions. They showed the influence of the wall temperature distribution on heat transfer

but they did not find a simple mathematical relation to express it. Afterwards, Yang et al. [6] found a new similarity solution of the boundary-layer equations for more complicated wall temperature distributions. Their conclusions were similar to those of Sparrow and Gregg, which confirmed that heat transfer is greatly affected by wall temperature distribution. They showed that the local temperature difference between the wall and the medium (ΔT) is not sufficient to determine the local heat flux. Classical correlation for a uniform value of ΔT along the wall cannot be used in such problems. Further, Semenov [7] derived the system of ordinary differential equations for all possible distributions of the wall and environment temperature leading to a similarity solution of the steady state boundary-layer equations. He chose the temperature difference at the leading edge of the wall as the characteristic temperature difference. Similarity transformations are limited to few specific cases, so research has been conducted in order to expand available solutions to include problems with non-similar surface conditions. Series expansion methods were used by Yang et al. [8] in the case of exponential and sinusoidal wall temperature distribution.

Another alternative for studying natural convection over a flat plate with an arbitrary temperature distribution is the use of numerical methods which are the most versatile for handling general boundary conditions [9]. Havet and Baly [10] studied turbulent natural convection over a vertical flat plate with the finite-volume method. They showed that buoyancy forces are locally affected by the slope of the temperature profile (S), and heat transfer is greatly influenced by wall temperature distribution.

The objective of the present work is to determine the influence of the non-uniformity of wall temperature on heat transfer by laminar natural convection over a vertical flat plate with a linearly varying temperature distribution into a supercritical fluid. The non-uniformity of wall temperature is defined by the slope of the temperature profile (S). We developed a numerical model based on a finite-difference formulation to solve the boundary-layer equation, and a complete parametric study was carried out in a laminar regime for different slopes of the wall temperature profile.

PROBLEM STATEMENT

The geometry and the coordinate system of the present problem are shown in Figures 1 and 2 where a vertical plate is depicted with a linear temperature distribution. The plate is immersed in a quiescent fluid, which is assumed to be maintained at a uniform temperature, and the fluid movement is entirely driven by buoyancy forces. In this problem the gravity acts in the negative x direction. The coordinate system is chosen such that

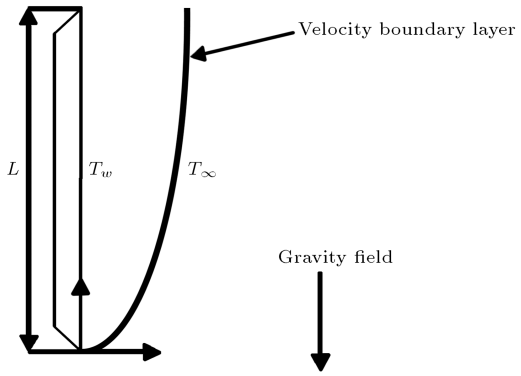

Figure 1. Geometry and coordinate system.

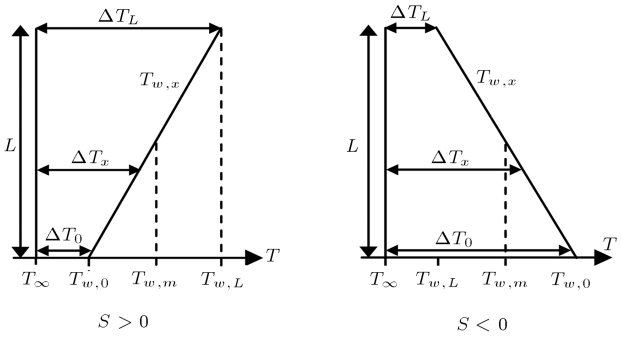

Figure 2. Wall and ambient temperature profiles according to S.

x measures the distance along the plate and y measures the distance normal to it. Far away from the plate, the velocity and the temperature of the uniform main stream are U_∞ and T_∞, respectively.

Assuming that the Boussinesq approximation is valid, the boundary-layer form of the governing equations which are based on the balance laws of mass, momentum and energy can be written as:

$$\frac{\partial u}{\partial x} + \frac{\partial v}{\partial y} = 0, \tag{1}$$

$$u\frac{\partial u}{\partial x} + v\frac{\partial u}{\partial y} = \beta g(T - T_\infty) + \gamma\frac{\partial^2 u}{\partial y^2}, \tag{2}$$

$$u\frac{\partial T}{\partial x} + v\frac{\partial T}{\partial y} = \alpha\frac{\partial^2 T}{\partial y^2}. \tag{3}$$

Here, u and v are the velocity components parallel and perpendicular to the plate, T is the temperature, β is the thermal expansion coefficient, γ is the kinematic viscosity, ρ is the fluid density, g is the acceleration due to gravity, and α is the thermal diffusivity.

The thermal expansion coefficient, which is used here, is not constant; a relation is derived for it as follows. Schmidt and Wenzel [11] presented a general form for cubic Equations Of State (EOS). Their equation is suitable at high pressures and temperatures such

as those encountered in processes with supercritical fluids. The equation is:

$$P = \frac{RT}{V' - b} - \frac{a}{V'^2 + u'bV' + wb^2}, \tag{4}$$

where:

$$Z = \frac{PV'}{RT}, \qquad A = \frac{aP}{(RT)^2}, \qquad B = \frac{bP}{RT}. \tag{5}$$

By simplifying Equation 4 for van der Waals gas;

$$Z^3 - (B+1)Z^2 + AZ - AB = 0, \tag{6}$$

the relation for β will be obtained as a function of the compressibility factor:

$$\beta = \frac{1}{T}\left[1 - \left(\frac{Z^2B - 2ZA + 3AB}{3Z^3 - 2Z^2(B+1) + ZA}\right)\right]. \tag{7}$$

The calculation of β involves two steps; first, the compressibility factor, Z, is determined by finding the appropriate root of Equation 6; then, Z is introduced into Equation 7 to obtain the value of β. It is interesting to verify that Equation 7 converges to $(1/T)$ at the ideal-gas limit. This limit is reached as $P \to 0$ at constant T.

$$P \to 0, \quad PV' \to RT,$$

i.e.:

$$Z \to 1 \text{ and } A \to 0, \quad B \to 0. \tag{8}$$

Therefore:

$$\beta = 1/T. \tag{9}$$

The appropriate boundary conditions for the velocity and temperature of this problem are as follows:

$$\begin{aligned} &y = 0; && u = 0, && v = 0, && T = T_W(x), \\ &y \to \infty; && u \to 0, && v \to 0, && T \to T_\infty, \\ &x = 0; && u = 0, && v = 0, && T = T_\infty. \end{aligned} \tag{10}$$

Equations 1 to 3 are coupled non-linear differential equations to be solved under the boundary conditions given in Equation 10. However, the exact analytical solutions are not possible for this set of equations, and hence we solve these equations by using the finite-difference method. After using appropriate dimensionless variables, the equivalent finite difference schemes corresponding to Equations 1 to 3 in dimensionless form are given by:

$$\left(-\frac{V_{i-1,j}}{2\Delta Y} - \frac{1}{\Delta Y^2}\right)U_{i,j-1} + \left(\frac{U_{i-1,j}}{\Delta X} + \frac{2}{\Delta Y^2}\right)U_{i,j} + \left(\frac{V_{i-1,j}}{2\Delta Y} - \frac{1}{\Delta Y^2}\right)U_{i,j+1} = \theta_{i-1,j}\beta + \frac{U_{i-1,j}^2}{\Delta X}, \tag{11}$$

$$\left(-\frac{V_{i-1,j}}{2\Delta Y} - \frac{1}{\mathrm{Pr}\Delta Y^2}\right)\theta_{i,j-1} + \left(\frac{U_{i-1,j}}{\Delta X} + \frac{2}{\mathrm{Pr}\Delta Y^2}\right)\theta_{i,j} + \left(\frac{V_{i-1,j}}{2\Delta Y} - \frac{1}{\mathrm{Pr}\Delta Y^2}\right)\theta_{i,j+1} = \frac{U_{i-1,j}\theta_{i-1,j}}{\Delta X}. \tag{12}$$

After some derivations, V values can be determined from the continuity equation as:

$$V_{i.j} = V_{i,j-1} - \left(\frac{\Delta Y}{2\Delta X}\right)(U_{i,j} - U_{i-1,j} + U_{i,j-1} - U_{i-1,j-1}). \tag{13}$$

Here, the index i refers to x and j to y. The above equations are explicit in the x-direction, while they are implicit in the y-direction. After specifying the conditions along some initial $i = 1$, U values and, in the following, θ values can be obtained on the $i = 2$ line. Then, V values are obtained on the $i = 2$ line. Having determined the values of all the variables on the $i = 2$ line, the same procedure can then be used to find the values on the $i = 3$ line and so on. More details on the numerical procedures can be found in the textbook by Oosthuizen and Naylor [12].

For the solution of the three coupled equations, an iterative procedure was used with an under-relaxation coefficient of 0.2 for a quicker convergence of the temperatures and velocities. Under-relaxation is generally used when the equations are non-linear. In this case, the relaxation coefficient must be between 0 and 1. This technique appears to be most appropriate when the convergence shows an oscillatory pattern and tends to overshoot the apparent final solution.

A mesh system with 150×150 nodes is proven to provide mesh-independent results. The heat-transfer coefficient, once the temperature field is obtained, as described above, is based on Equation 14:

$$h_x = -\frac{k}{(T_w - T_\infty)}\left(\frac{\partial T}{\partial y}\right)_{y \to 0}. \tag{14}$$

Once h_x is obtained, the following dimensionless numbers are computed:

$$\mathrm{Nu}_x = \frac{h_x x}{k}, \qquad \mathrm{Ra}_x = \frac{\beta_{\mathrm{ref}} g(T_w - T_\infty)x^3}{\gamma\alpha}. \tag{15}$$

ESTIMATION OF FLUID PROPERTIES

Viscosity Estimation

The procedure used to estimate the viscosity of the fluids at supercritical conditions was given in Poling et al. [13]. This method is recommended for dense fluids at super- or near-critical conditions. In this reference the product $\xi\eta$ is presented as a function of reduced temperature (T_r) where η is the dynamic viscosity in (Pa.s) and ξ is defined as:

$$\xi = 0.176 \left(\frac{T_c}{M^3 P_C^4} \right)^{1/6}, \tag{16}$$

where T_c is in (K), P_c in (bar), and M in (g/mol).

Note that ξ is a unique property of each fluid that does not depend on T or P.

Thermal Conductivity Correlation

The method used in this work is the one proposed by Stiel and Thodos [14]. They used a dimensional analysis to obtain a correlation between $k - k^0$, Z_c, Γ and ρ. Then, they established the following approximate analytical expressions:

$$k = \begin{cases} k^0 + \frac{1.22\times10^{-2}[\exp(0.535\rho_r)-1]}{\Gamma Z_c^5} & 0<\rho_r<0.5 \\ k^0 + \frac{1.14\times10^{-2}[\exp(0.67\rho_r)-1.069]}{\Gamma Z_c^5} & 0.5<\rho_r<2.0 \\ k^0 + \frac{2.6\times10^{-3}[\exp(1.155\rho_r)+2.016]}{\Gamma Z_c^5} & 2.0<\rho_r<2.8 \end{cases} \tag{17}$$

where k^0 is the ideal-gas or low-pressure limit of the thermal conductivity and ρ_r is the reduced density which was calculated in this work as:

$$\rho_r = \frac{3}{8}\frac{PT_c}{ZT_f P_c}, \tag{18}$$

and Γ is a parameter defined by:

$$\Gamma = 210 \left(\frac{T_c M^3}{P_c} \right)^{1/6}, \tag{19}$$

where k^0 is in (W/m.K), T in (K), P_c in (bar) and M in (g/mol).

Heat Capacity Approximation

The heat capacities of real gases are related to the corresponding values in the ideal-gas or low-pressure state (at the same temperature and composition) by the following definition:

$$C_p = C_p^0 + \Delta C_p, \tag{20}$$

where ΔC_p is the so-called residual heat capacity. (This definition can be applied to a pure gas or to a gas mixture at constant composition.) The residual heat capacity can be estimated from the Lee-Kesler [15] correlation as a function of T_r and P_r:

$$\Delta C_p = C_p - C_p^0 = (\Delta C_p)^0 + \omega(\Delta C_p)^1. \tag{21}$$

RESULTS AND DISCUSSION

In this part, the results of the thermal expansion coefficient (β) are presented, based on the thermodynamic model and the van der Waals Equation Of State (EOS). These values are presented graphically where they are compared with the ideal-gas and reference values. For butane, the calculations were carried out at three different pressures: 1.80 MPa, 3.796 MPa (P_c) and 5.50 MPa. For carbon dioxide, the pressures used were: 3.69 MPa (0.5 P_c), 7.38 MPa (P_c) and 10 MPa. Figure 3 represents three isobars of β versus T for carbon dioxide where the calculated values are compared with the reference values [16] and ideal gas assumption ($\beta = 1/T_f$). It can be seen that the van der Waals equation of state, despite its simplicity, does provide an excellent representation of the data. Also interesting is the fact that thermal expansivity (β) diverges at the critical point ($T_r = 1$, $P_r = 1$) and this happens regardless of the Equation Of State (EOS) used. The critical temperature for butane and carbon dioxide is 425.16 (K) and 304.10 (K), respectively.

It is well known that β for liquids at low (atmospheric) pressure increases with temperature, while the opposite is true for low-pressure gases. Higher-pressure isobars show a liquid-like behavior at lower (subcritical) temperatures, a gas-like behavior at higher (supercritical) temperatures and a maximum at an intermediate temperature, close but not necessarily equal to T_c. At even higher temperatures, all isobars approach the ideal-gas behavior.

In Figure 4, the results of the present study (Variable wall temperature) and Ref. [17] (constant wall temperature) are compared and it is observed that there is a good agreement between both solutions. This figure indicates that the variable wall temperature does not affect β values significantly.

Figure 5 shows similar plots for butane where the qualitative observations presented above for carbon dioxide apply equally well to the butane. We also solved the problem for other fluids like water, propane and other solvents that are applicable in supercritical processes, and there was good agreement between the results. The results of carbon dioxide and butane are presented here for brevity. For both substances, carbon dioxide and butane, the ideal-gas thermal expansion coefficient was calculated as the inverse absolute temperature. The experimental results of the thermal

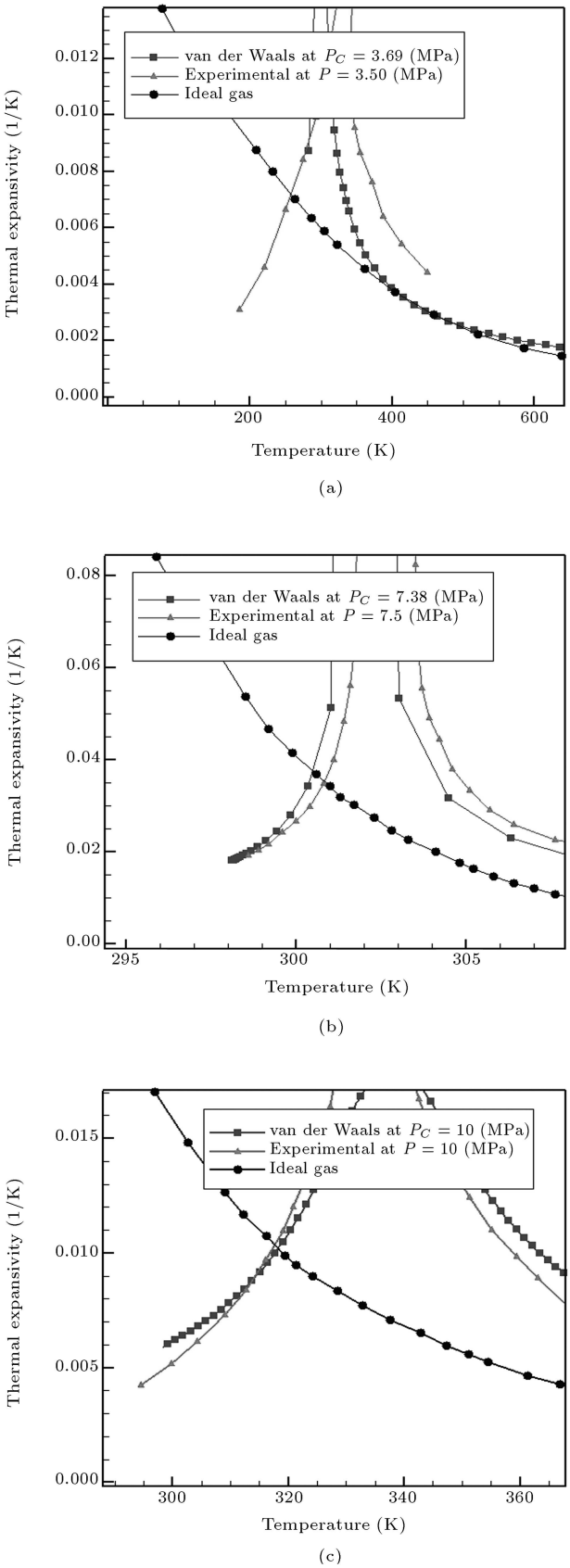

Figure 3. Thermal expansion coefficient of carbon dioxide at (a) $P = 3.69$ (MPa) (0.5 P_c), (b) $P = 7.38$ (MPa) (P_c), and (c) $P = 10$ (MPa), reproduced after [17].

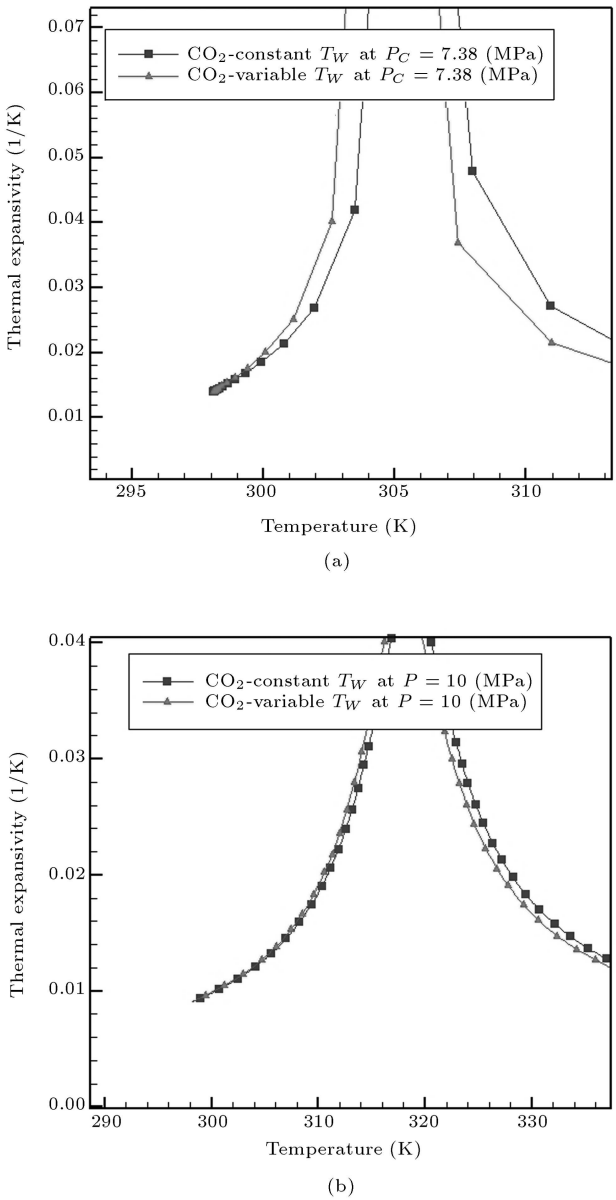

Figure 4. Thermal expansion coefficient of carbon dioxide at (a) $P = 7.38$ (MPa), and (b) $P = 10$ (MPa) for variable and constant wall temperature (T_w).

expansivity coefficient for liquid butane were taken from Haynes and Goodwin [18].

In this study, our main objective is to determine the influence of the non-uniform wall temperature distribution on heat transfer. We focused on the case of a linearly wall temperature distribution, characterized by slope S. Both negative and positive S values were investigated. The Nusselt number values computed as a function of the Rayleigh number for supercritical carbon dioxide with a variable thermal expansivity coefficient, and are shown in Figure 6. The simulations were performed at $P_r = 1.05$ and $T_r = 1.05$. The results of these simulations are plotted in a logarithmic scale so that the curves approach straight lines. It is ob-

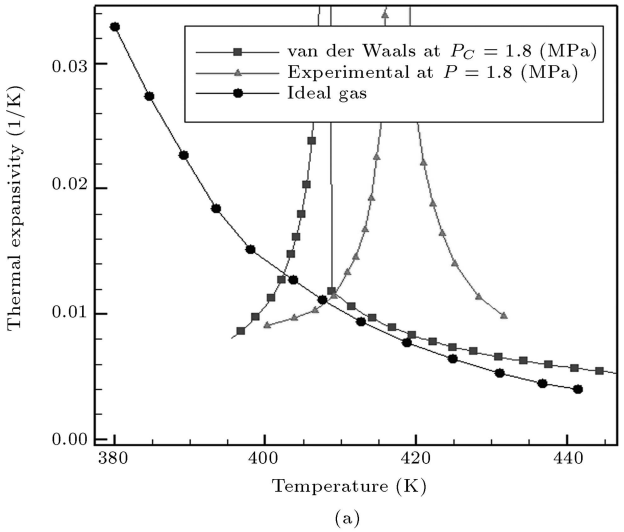

(a)

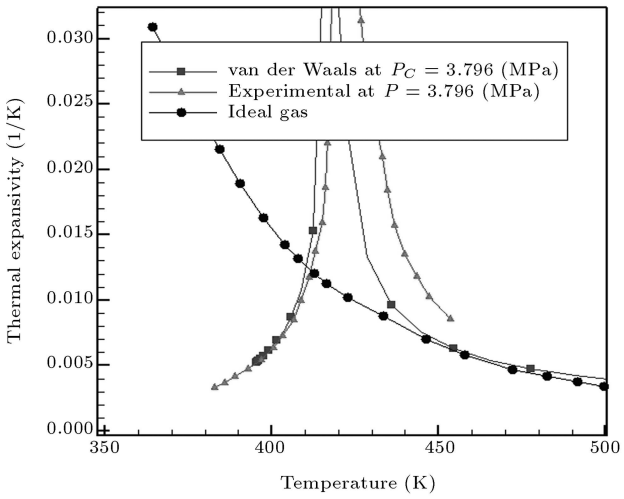

(b)

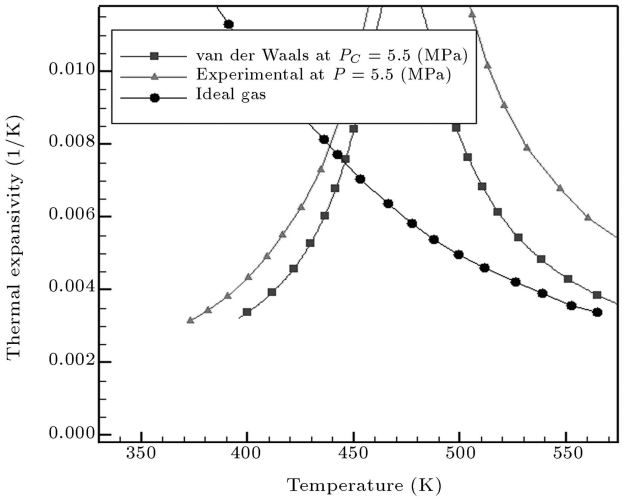

(c)

Figure 5. Thermal expansion coefficient of butane at (a) = 1.8 (MPa), (b) = 3.796 (MPa) (P_c), and (c) = 5.5 (MPa).

served that a positive slope of temperature distribution ($S > 0$) will increase heat transfer rate and a negative one ($S < 0$) will decrease it. It is also interesting to note that by increasing the slope, the heat transfer rate will rise gradually.

For comparing the obtained results and results of [17], Nusselt versus Rayleigh is illustrated in Figure 7 for carbon dioxide at $P_r = 1.05$ and $T_r = 1.20$. It is observed from the graph that the heat transfer rate for variable temperature increases, in comparison with a constant temperature under the same condition. The curve corresponding to the empirical correlation is obtained from a relation that was proposed by Churchill and Chu [19], and is applicable over a wide

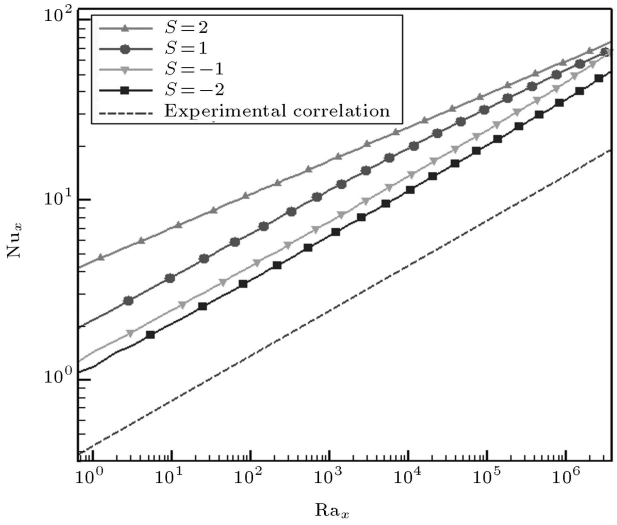

Figure 6. Nu_x as a function of Ra_x at $P_r = 1.05$ and $T_r = 1.05$ for carbon dioxide.

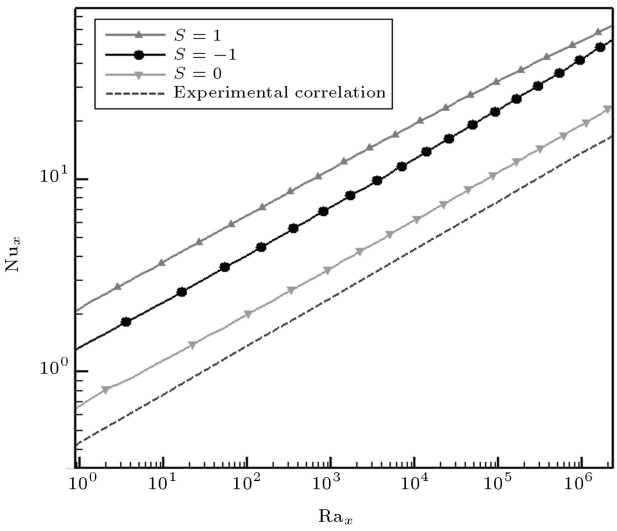

Figure 7. Nu_x as a function of Ra_x at $P_r = 1.05$ and $T_r = 1.2$ for carbon dioxide, variable and constant wall temperature (T_w).

range of Rayleigh numbers. This is:

$$\mathrm{N\bar{u}}_L = 0.68 + \frac{0.670\mathrm{Ra}_L^{1/4}}{[1+(0.492/\mathrm{Pr})^{9/16}]^{4/9}},$$

$$\text{for } 0 < \mathrm{Ra}_L < 10^9. \tag{22}$$

Figure 8 shows Nu_x as a function of Ra_x for butane at $P_r = 1.05$ and $T_r = 1.05$. The same trend shown in Figure 6 is observed here, and also it can be seen that for Ra$> 10^6$ numbers, the results of positive and negative slopes reach each other.

The influence of the slope S parameter on velocity and temperature profiles, as well as on the Nusselt number, is also determined. For illustration purposes, the velocity profiles for variable and constant thermal expansivity for butane, at an arbitrarily chosen value of x, are plotted in Figure 9. The values of u were obtained at $x = 0.04185$ (m) for $P_r = 1.05$ and $T_r = 1.05$.

It is observed that the thickness of the boundary layer at a variable temperature is much higher than in a constant temperature case and this thickness for a positive slope is greater than for a negative one. Note that the velocity profile with variable thermal expansivity has a much high maximum velocity than the one with constant thermal expansivity. The velocity maximum is at the heart of all these lines and the velocity gradually approaches zero, outside the boundary layer.

Figure 10 shows the dimensionless temperature profiles at the same conditions of Figure 9. This figure confirms that the boundary layer for a variable wall temperature is greater than for a constant wall temperature, and it is also indicated that the boundary layer for variable thermal expansivity is thinner than that for constant thermal expansivity.

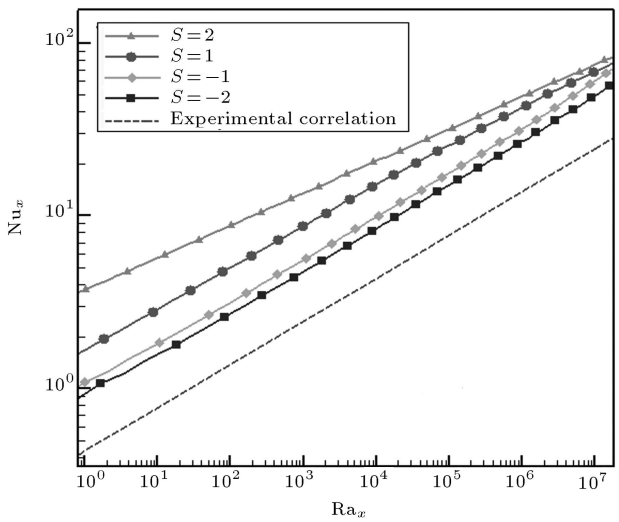

Figure 8. Nu_x as a function of Ra_x at $P_r = 1.05$ and $T_r = 1.05$ for butane.

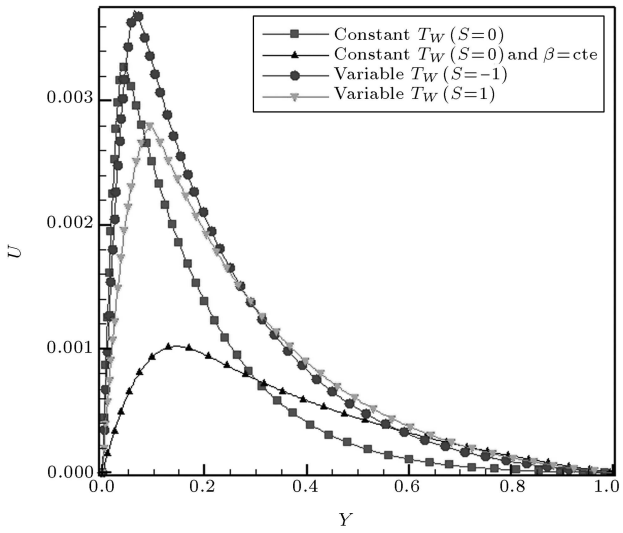

Figure 9. Dimensionless velocity profile for butane at $x = 0.04185$ (m) for $P_r = 1.05$ and $T_r = 1.05$.

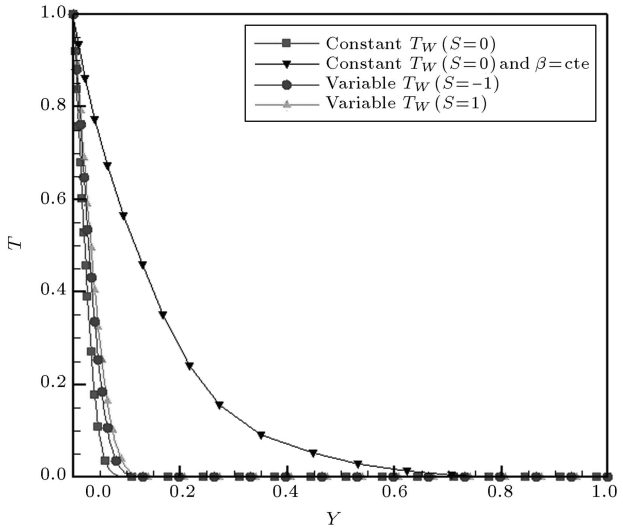

Figure 10. Dimensionless temperature profile for butane at $x = 0.04185$ (m) for $P_r = 1.05$ and $T_r = 1.05$.

It should also be noted that the agreement is very good if the velocity and temperature profiles obtained with a numerical code at constant thermal expansivity are compared with those given in classical text books like [20].

CONCLUSION

A thermodynamic model has been developed to represent the thermal expansivity of real fluids based on an equation-of-state approach. This contribution is important in various regards. First, in any practical application of supercritical fluid extraction where heat transfer plays a role, the effect of free convection has to be taken into account because of the considerable enhancement of this phenomenon in the supercritical

region of the solvent. Second, when developing a model or correlation for free convection, it is normally assumed that β is a constant. In view of the results presented here, when working near the critical point of the solvent, this assumption is no longer valid.

A numerical model was developed for the analysis of the free-convection flow over a vertical flat plate with variable thermal expansivity and variable wall temperature. The numerical simulations were performed for two fluids: carbon dioxide and butane.

According to the nature of the problem, the velocity and temperature profiles make sense and a logical trend is observed in the obtained graphs. They also imply that the thickness of the boundary layer at variable temperature is much higher than at constant temperature, wherein the thickness for the positive slope is greater than for the negative one. Also, velocity and temperature profiles were plotted at constant thermal expansivity, showing good agreement with the values reported in existing literature. The results were expressed in terms of dimensionless numbers as local Nusselt and Raleigh numbers. It was found that a positive slope of temperature distribution ($S > 0$) will increase the heat transfer rate, and a negative one ($S < 0$) will decrease the heat transfer rate.

NOMENCLATURE

Roman Symbols

a, b	EOS constants that correct for intermolecular attractive forces ($\mathrm{N.m^4/mol^2}$)
A, B	dimensionless EOS parameters (-)
C_p	heat capacity of the fluid (J/kg.K)
C_p^0	heat capacity at the low-pressure limit (J/kg.K)
g	local acceleration of gravity ($\mathrm{m/s^2}$)
Gr_w	Grashof number (-)
h_x	local heat-transfer coefficient ($\mathrm{W/m^2.K}$)
k	thermal conductivity of the fluid (W/m.K)
k^0	thermal conductivity at the low-pressure limit (W/m.K)
L	height of the vertical plate (m)
M	molecular weight of the fluid (kg/mol)
Nu	Nusselt number (-)
Nu_x	local Nusselt number (-)
P, P_c	pressure and critical pressure, respectively (Pa)
$P_r = P/P_c$	reduced pressure (-)
Pr	Prandtl number (-)
R	gas constant (J/mol.K)
Ra_L	Rayleigh number based on the length of the plate (-)
T, T_c	temperature and critical temperature, respectively (K)
S	slope of the wall temperature linear distribution
ρ	density of the fluid ($\mathrm{kg/m^3}$)
ρ_r	reduced density (-)
ω	acentric factor (-)
T_f	fluid average temperature (K)
$T_r = T/T_c$	reduced temperature (-)
T_w	wall temperature of the vertical flat plate (K)
T_∞	fluid medium temperature (K)
u, v	velocity component in the x, y direction, respectively (m/s)
V'	molar volume ($\mathrm{m^3/mol}$)
V_c	critical molar volume ($\mathrm{m^3/mol}$)
u', w	EOS parameters (-)
U, V	dimensionless velocity components in the x, y direction, respectively (-)
x, y	coordinates parallel and normal to the vertical, plate, respectively, (m)
X, Y	dimensionless coordinate parallel and normal to the vertical plate, respectively (-)
Z	compressibility factor (-)
Z_c	critical compressibility factor (-)

Greek Symbols

α	thermal diffusivity ($\mathrm{m^2/s}$)
β	thermal expansion coefficient (1/K)
ν	kinematic viscosity ($\mathrm{m^2/s}$)
Γ	inverse thermal conductivity (m.K/W)
θ	dimensionless temperature (-)
ξ	inverse viscosity ($\mathrm{m^2/N.s}$)

Subscripts

i	node index in the x direction
j	node index in the y direction
P	constant pressure
∞	outside the boundary layer

REFERENCES

1. Arai, Y., Sako, T. and Takebayashi, Y., *Supercritical Fluids-Molecular Interactions, Physical Properties and*

New Applications, First Ed., Springer, Berlin, Germany (2001).

2. Ostrach, S. "An analysis of laminar free-convection flow and heat transfer about a flat plate parallel to the direction of the generating body force", Report 1111-Supersedes NACA TN 2635 (1952).
3. McHugh, M.A. and Krukonis, V.J., *Supercritical Fluid Extraction: Principles and Practice*, Butterworth, Heinemann (1994).
4. Nishikawa, K. and Ito, T. "An analysis of free-convective heat transfer from an isothermal vertical plate to supercritical fluid", *Int. J. of Heat and Mass Transfer*, **12**, pp. 1449-1463 (1969).
5. Sparrow, M. and Gregg, J.L. "Similar solutions for free convection from a non-isothermal vertical plate", *Transactions of the ASME*, **80**, pp. 379-386 (1958).
6. Yang, K.T., Novotny, J.L. and Cheng, Y.S. "Laminar free convection from a non-isothermal vertical plate immersed in a temperature stratified medium", *Transactions of the ASME*, **80**, pp. 1097-1109 (1972).
7. Semenov, V.I. "Similar problems of steady-state laminar free convection on a vertical plate", *Heat Transfer, Sov. Research*, **16**, pp. 67-85 (1984).
8. Yang, J., Jeng, D.R. and De Witt, K.J. "Laminar free convection from a vertical plate with non uniform surface conditions", *J. of Numerical Heat Transfer*, **5**, pp. 165-184 (1982).
9. Merkin, J.H. and Pop, I. "Conjugate free convection on a vertical surface", *Int. J. of Heat and Mass Transfer*, **39**(7), pp. 1527-1534 (1996).
10. Havet, M. and Blay, D. "Natural convection over a non-isothermal vertical plate", *Journal of Heat Transfer*, **42**, pp. 1410-1424 (1999).
11. Schmidt, G. and Wenzel, H. "Free convection with suction and blowing", *J. of Chemical Engineering Science*, **35**, p. 1503 (1980).
12. Oosthuizen, P. and Naylor, D., *An Introduction to Convective Heat Transfer Analysis*, First Ed., McGraw-Hill, New York (1999).
13. Poling, B., Prausnitz, J. and O'Connell, J., *The Properties of Gases and Liquids*, Fifth Ed., McGraw-Hill, New York (2001).
14. Stiel, L.I. and Thodos, G. "Natural convection in a thermally stratified fluid", *J. of AIChE*, **10**, p. 26 (1964).
15. Lee, B.I. and Kesler, M.G. "A theoretical analysis of laminar natural convection heat transfer to non-Newtonian liquids", *J. of AIChE*, **21**, p. 510 (1975).
16. Angus, S., Armstrong, B. and Reuck, K., *International Thermodynamic Tables of the Fluid State-Carbon Dioxide*, First Ed., Pergamon Press, Headington Hill Hall, Oxford OX3 0BW, England (1976).
17. Rolando, C. "Natural convection in supercritical fluids", M.Sc. Thesis, University of Puerto Rico, Greece (2004).
18. Haynes, W.M. and Goodwin, R.D., *Thermophysical Properties of Normal Butane from 135 to 700 K at Pressures to 70 MPa*, U.S. Department of Commerce., U.S. Government Printing Office, Washington, DC (1982).
19. Churchill, S.W. and Chu, H.H.S. "Correlation equations for laminar and turbulent free convection from a vertical plate", *Int. J. of Heat Mass Transfer*, **18**, p. 1323 (1975).
20. Bejan, A., *Convection Heat Transfer*, First Ed., John Wiley & Sons, New York (1984).